New Phytologist

***New Phytologist* Supporting Information**

Article title: **A non-DNA-binding activity for the ATHB4 transcription factor in the control of vegetation proximity**

Authors: Marçal Gallemí, Maria Jose Molina-Contreras, Sandi Paulišić, Mercè Salla-Martret, Céline Sorin, Marta Godoy, Jose Manuel Franco-Zorrilla, Roberto Solano, Jaime F. Martínez-García.

Article acceptance date: 29 June 2017

The following Supporting Information is available for this article:

Fig. S1 Phenotypic analyses of seedlings over-expressing *ATHB2*, *HAT2*, *HAT1*, *HAT2-GR*, *ATHB4-GFP* and *ATHB4-GR*.

Fig. S2 Evaluation of biological relevance of DNA-motifs from co-regulation information.

Fig. S3 Analysis of the homodimerization activity of the HD-Zip region of ATHB4.

Fig. S4 Subcellular localization of ATHB4 and its derivatives.

Fig. S5 Phenotypic analyses of seedlings over-expressing *ATHB4-GR*.

Fig. S6 Levels of transgene expression in ATHB4-derivative truncated lines.

Fig. S7 $ATHB4_{N210A}$ is impaired in DNA-binding.

Fig. S8 Detection of GFP-fused proteins in two transgenic ATHB4 derivative lines.

Fig. S9 ATHB4 promotes upwards leaf curling.

Table S1 Primers used for amplifying and cloning genes used in this work.

Table S2 Primers used for qPCR analyses.

Table S3 Overlap of bioset of DEX-regulated genes in –CHX and +CHX treated 35S:ATHB4-GR (pCS19) seedlings, BH<0.05, FC≥1.5.

Table S4 ATHB4-interacting proteins identified in the Y2H screen.

New Phytologist

Methods S1 Generation of GFP- and GR-fused constructs for plant transformation.

Methods S2 Transcriptomic analyses.

Methods S3 Gene expression analysis by RNA blot analysis.

Methods S4 Yeast Two Hybrid (Y2H) assays.

Methods S5 Subcellular localization analyses.

Methods S6 Expression of recombinant ATHB4-MBP for Protein Binding Microarrays (PBMs).

Methods S7 Chromatin immunoprecipitation (ChIP).

Methods S8 Protein extraction and immunoblot analyses.

References

Fig. S1 Phenotypic analyses of seedlings over-expressing *ATHB2*, *HAT2*, *HAT1*, *HAT2-GR*, *ATHB4-GFP* and *ATHB4-GR*. **(A)** Cartoon describing the growth conditions employed to analyze the response to simulated shade. Wild-type (Col-0) and transgenic seedlings were germinated and grown for 2 days in continuous W light in media supplemented without (–DEX) or with the indicated amount of DEX (+DEX) and then either kept in W or transferred to W+FR for 5 more days. Hypocotyl length of Col-0, 35S:ATHB2, 35S:HAT2 **(B)**, two independent transgenic lines of 35S:HAT1 **(C)** and 35S:ATHB4-GFP **(D)** seedlings grown as indicated in **A**. **(E)** Hypocotyl length of Col-0 and 35S:ATHB4-GR seedlings grown in –DEX or increasing concentrations of DEX, as indicated in **A**. **(F)** Hypocotyl length of Col-0 and three independent transgenic lines of 35S:HAT2-GR seedlings grown in –DEX or + 5 µM DEX media, as indicated in **A**. In **B-F**, columns represent the mean ± SE. In **B-D** and **F**, asterisks indicate significant differences (**P<0.01) relative to the wild type control growing in the same conditions. In **E**, asterisks indicate significant differences (*P<0.05, **P<0.01) relative to the same genotype growing in the same light conditions without DEX (–DEX).

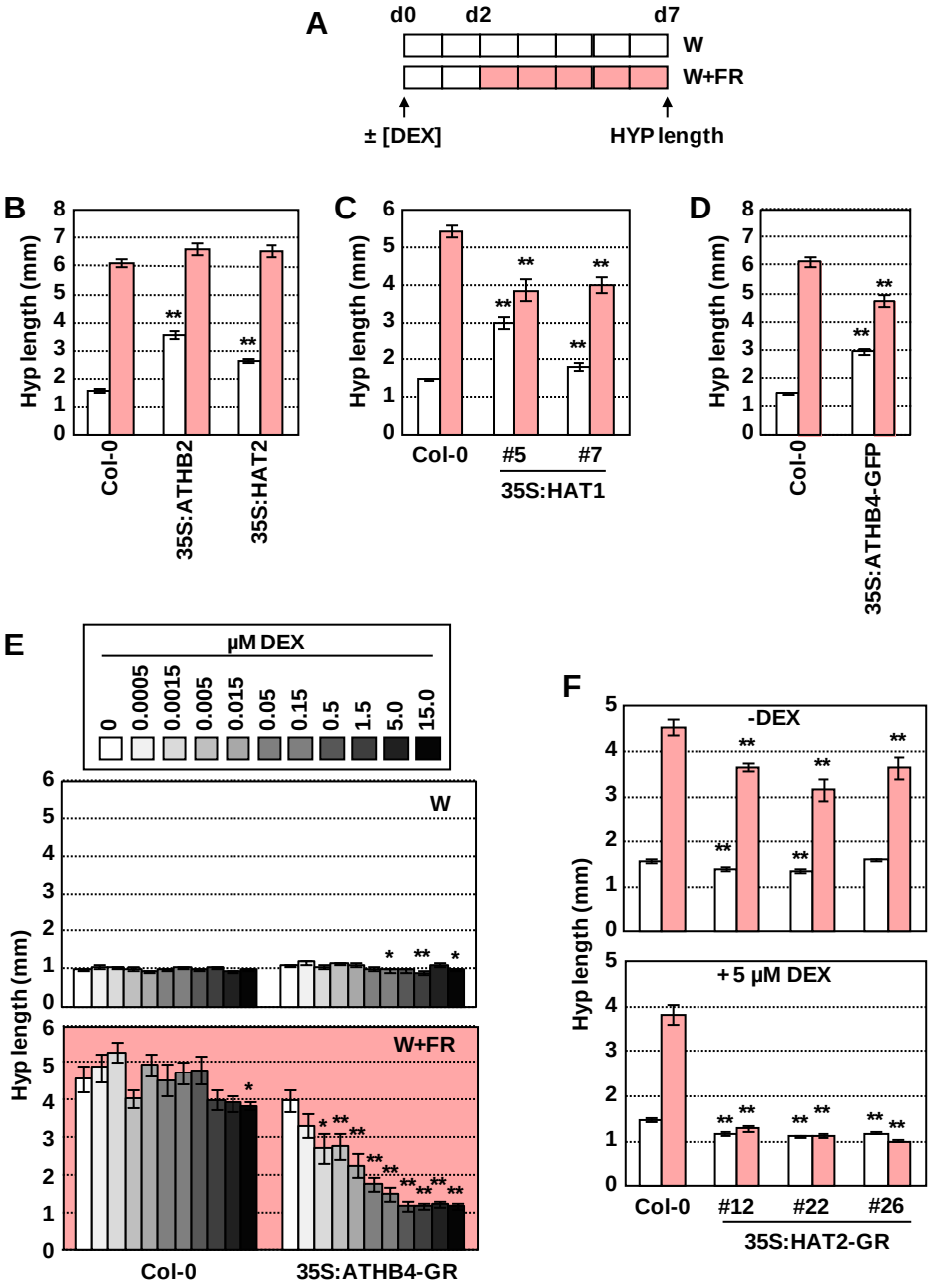
A
d0
d2
d7
W
W+FR
± [DEX]
HYP length
B
Hyp length (mm)
Col-0
35S:ATHB2
35S:HAT2
C
Hyp length (mm)
Col-0
#5
#7
35S:HAT1
D
Hyp length (mm)
Col-0
35S:ATHB4-GFP
E
µM DEX
0
0.0005
0.0015
0.005
0.015
0.05
0.15
0.5
1.5
5.0
15.0
W
W+FR
Hyp length (mm)
Col-0
35S:ATHB4-GR
F
-DEX
+ 5 µM DEX
Hyp length (mm)
Col-0
#12
#22
#26
35S:HAT2-GR

Fig. S2 Evaluation of biological relevance of DNA-motifs from co-regulation information. Lists of co-regulated genes with ATHB4 were scanned for the presence of ATHB4 target sequences at their promoter regions (1 kb). Frequencies (in %) of positively (blue bars) and negatively (red bars) co-regulated genes containing the indicated DNA elements are shown. Proportions of genes represented in the ATH1 microarray containing the corresponding elements, and thus representing a random distribution, are represented as green bars. Asterisks indicate the degree of statistical significance in the differences of the proportions indicated (*P < 0.05; **P < 0.01).

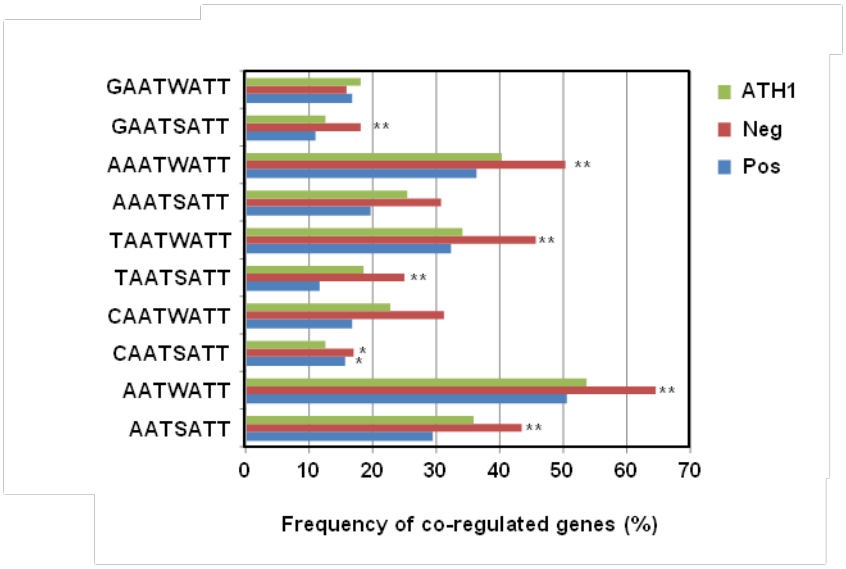

Fig. S3 Analysis of the homodimerization activity of the HD-Zip region of ATHB4. **(A)** Alignment of the amino acid sequences of ATHB2 and ATHB4. Arrows indicate the limits of the HD and Zip domains in ATHB2 proposed by different authors: (1) (Schena & Davis, 1992); (2) (Schena *et al.*, 1993); (3) (Sessa *et al.*, 1993); and (4) (Carabelli *et al.*, 1993). Colored boxes depict the chosen limits on the amino acid sequence of ATHB4 of the HD (H, orange) and Zip (Z, lilac) domains, and the adjacent N-terminal (N, yellow) and C-terminal (C, green) regions. **(B)** Experimental design of the specific combinations of BD and AD yeast constructs used in the yeast two hybrid assays. **(C)** Dilution spots of the yeast strains described in **B**. SD-LW and SD-AHLW refer to the selective media indicative of transformed cells or interaction between the hybrid proteins, respectively. All transformations were repeated at least twice with identical results. Empty vectors and truncated forms of murine p53 (in pVA3) and SV40 large T-antigen (in pTD1), known to interact, are used as negative (#4) and positive (#5) controls in this growth assay, respectively.

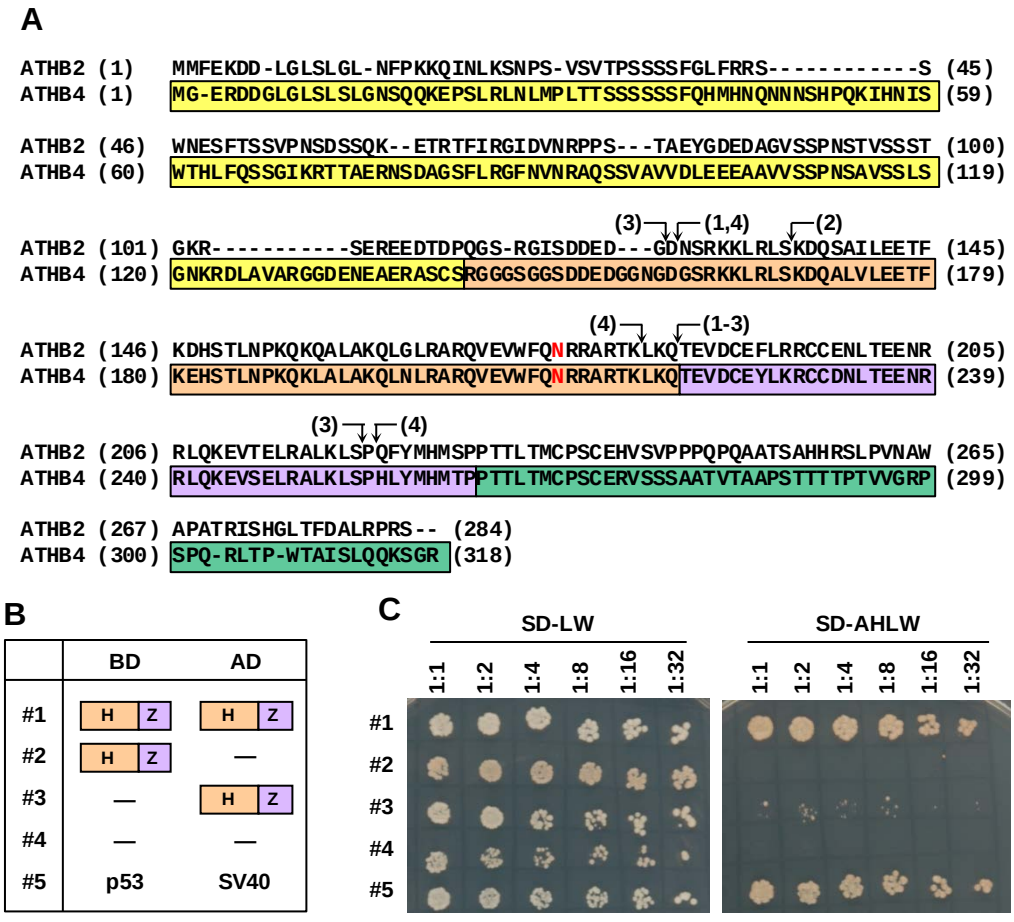

Fig. S4 Subcellular localization of ATHB4 and its derivatives. **(A-I)** Onion epidermal cells were co-bombarded with a GFP-containing construct and DsRed, a Red Fluorescent Protein (RFP) used as transformation control. Green (left) and red (right) fluorescences was analyzed after 24 h. Panels are shown to the same scale. Bar = 50 µm. **(J)** Alignment of HAT1, HAT2, HAT3, ATHB2 and ATHB4 amino acid sequences around the predicted NLS identified *in silico* in ATHB4 (highlighted in red).

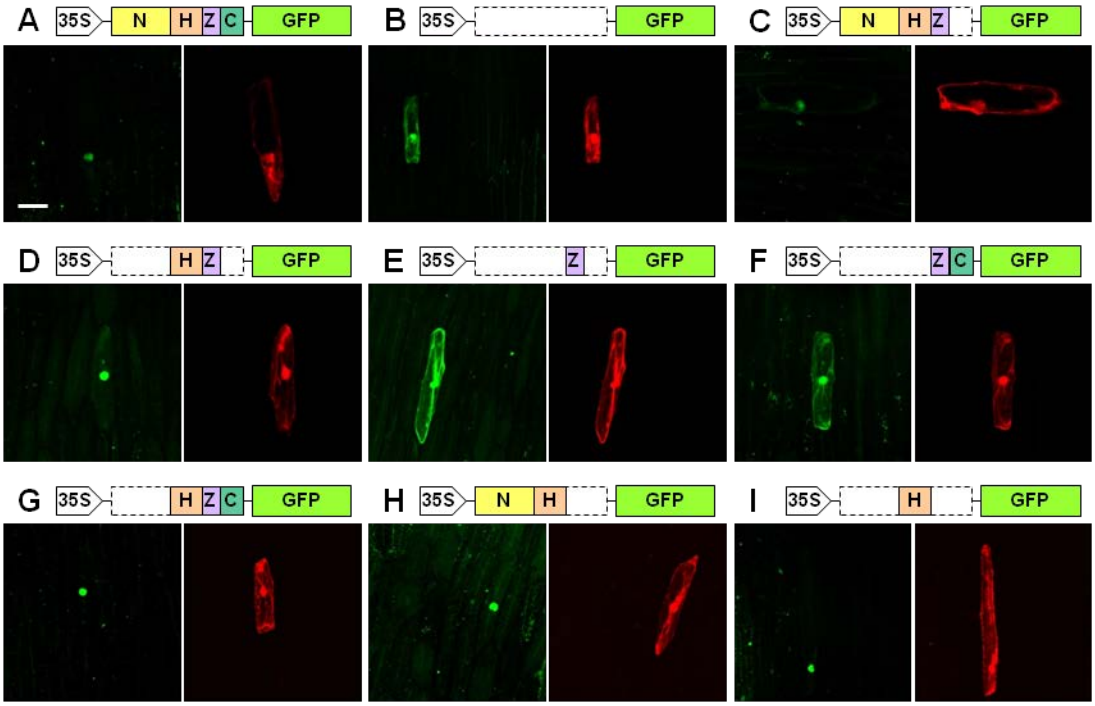

J

```
ATHB4  G-DGSRKKLRLSKDQ
HAT3   GDDSSRKKLRLSKEQ
ATHB2  G-DNSRKKLRLSKDQ
HAT1   GGETCRKKLRLSKDQ
HAT2   GGETSRKKLRLSKDQ
```

Fig. S5 Phenotypic analyses of seedlings over-expressing *ATHB4-GR*. **(A)** Cartoon describing the growth conditions employed to analyze the response to simulated shade. Wild-type (Col-0) and 35S:ATHB4-GR seedlings were germinated and grown for 2 days in continuous W light in media supplemented without (–DEX) or with DEX (+DEX) and then either kept in W or transferred to W+FR for 5 more days. **(B)** Aspect of 7-day-old grown seedlings grown as indicated in **A**. Seedlings are shown to the same scale. **(C)** Hypocotyl length of seedlings grown as indicated in **A**. Columns represent the mean ± SE. Symbols indicate significant differences (**P<0.01) relative to the wild type control growing in the same conditions. **(D)** Ratio of hypocotyl lengths of +DEX and –DEX seedlings growing in W and W+FR calculated from data shown in **C**. Asterisks indicate significant differences (**P<0.01) relative to the control.

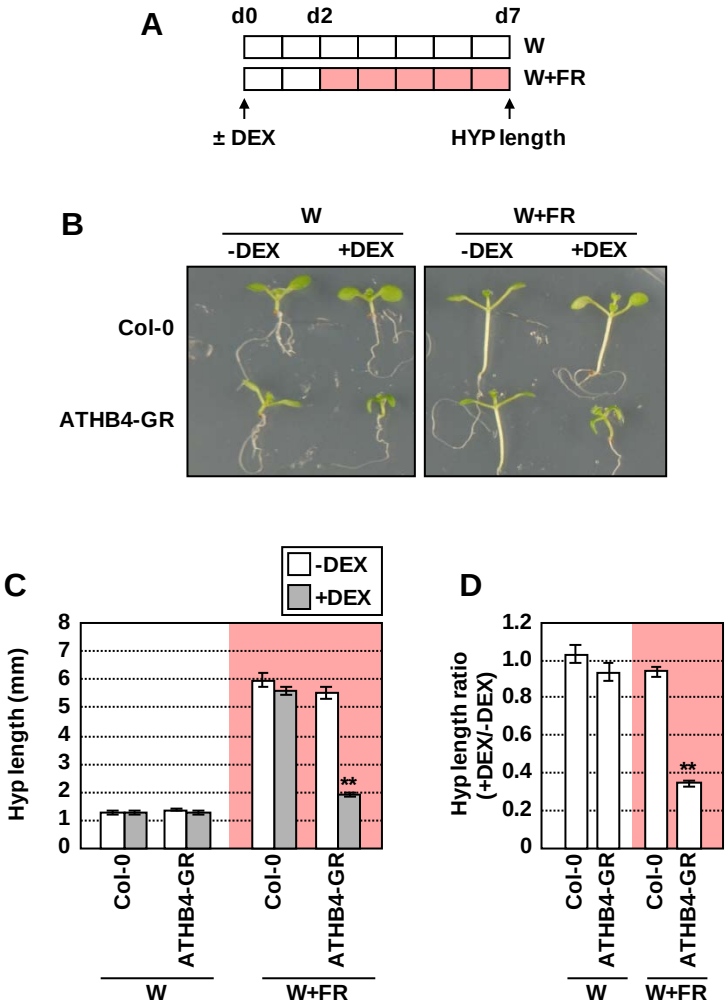

Fig. S6 Levels of transgene expression in ATHB4-derivative truncated lines. **(A)** Transcript abundances of *GR* genes, normalized to *UBQ10*, are shown in the indicated transgenic lines. Gene expression is presented relative to the levels of the analyzed gene in 35S:ATHB4-GR seedlings without DEX treatment. Values are means ± SE of three independent RT-qPCR biological replicates. Transgene transcript levels were quantified by RT-qPCR using specific GR primers in the same samples shown in Figure 3B-F. Asterisks indicate significant differences in transcript levels (Student *t* test, *P<0.05, **P<0.01) relative to the 35S:ATHB4-GR line grown under the same DEX treatment. **(B)** Cartoon describing the growth conditions (left side) employed to analyze the expression levels of the transgene in the 00Z0-GR and 0H00-GR lines (right side). T2 generation seedlings were germinated and grown for 7 days in continuous W light in media without DEX (–DEX). Transgene transcript levels were analyzed by Northern-blot.

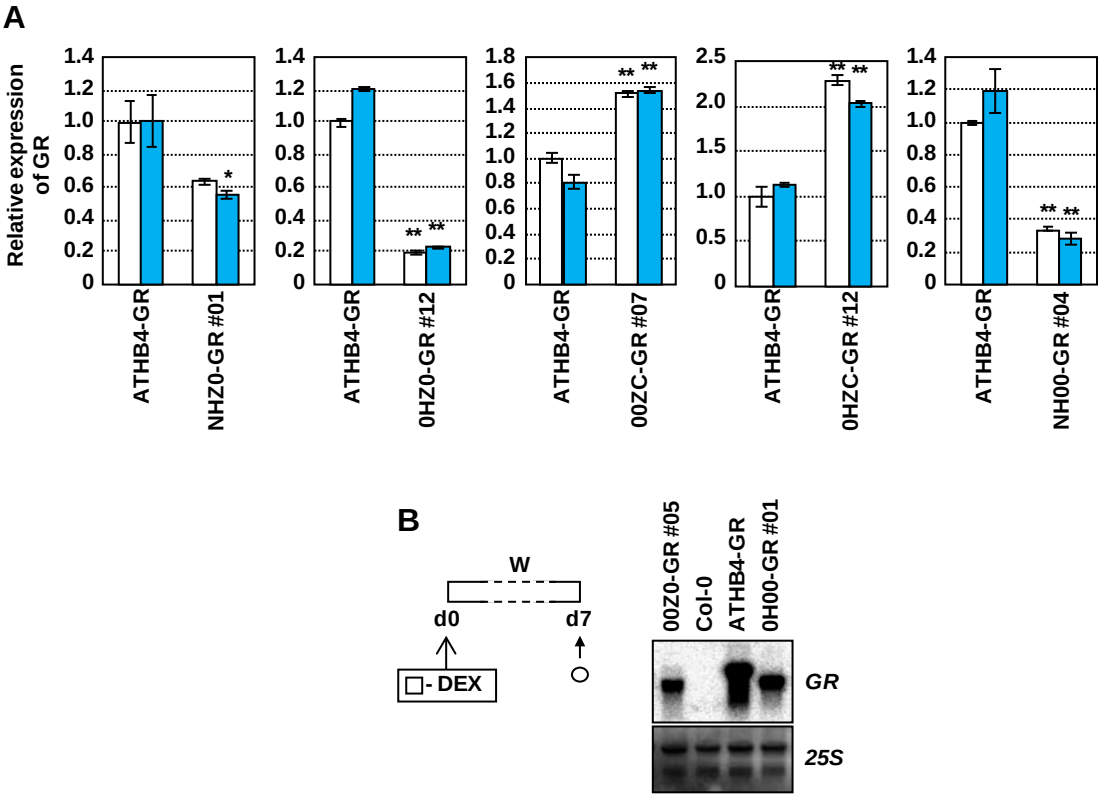

Fig. S7 ATHB4$_{N210A}$ is impaired in DNA-binding. **(A-B)** E-score for top scoring 8-mer consensus sequences preferentially bound by ATHB4 and ATHB4$_{N210A}$. **(C, D)** DNA-binding specificity of ATHB4 **(C)** and ATHB4$_{N210A}$ **(D)**. Position weight matrix (PWM) representation of the top scoring 10-mer consensus sequences preferentially bound by ATHB4 and ATHB4$_{N210A}$. **(E, F)** Transcript abundances of *GR* genes, normalized to *UBQ10*, are shown in the indicated transgenic lines. Gene expression is presented relative to the levels of the analyzed gene in 35S:ATHB4-GR seedlings without DEX treatment. Values are means ± SE of three independent RT-qPCR biological replicates. Transgene transcript levels were quantified by RT-qPCR using specific GR primers in the same samples shown in Figure 4E-F. Asterisks indicate significant differences in transcript levels (Student *t* test, *P<0.05, **P<0.01) relative to the 35S:ATHB4-GR line grown under the same DEX treatment.

A

ATHB4	E-score
CAATGATT	0.49686
TAATCATT	0.49547
CCAATCAT	0.49514
CTAATCAT	0.49455
CAATCATA	0.49447
CAATCATT	0.49434
TCAATCAT	0.49432
CAATAATT	0.49398
GCAATCAT	0.49333
TAATCATA	0.49328
AATCATTA	0.49306
TAATTATT	0.49294
CCAATGAT	0.49215
AAATCATT	0.49179
ATGATTAC	0.49166

B

ATHB4$_{N210A}$	E-score
TTAATTAA	0.41773
TAATTAAA	0.40624
AATTAAAT	0.40039
ATAATTAT	0.39965
AATCAAAT	0.39776
CATTAATT	0.39275
ATTTAAAT	0.39188
AATTTAAT	0.39130
TATTTAAA	0.38898
AAATTAAT	0.38876
CAATTAAT	0.38875
ATATTAAT	0.38814
ATTATCAT	0.38695
TGATAATT	0.38673
GTATAATT	0.38635

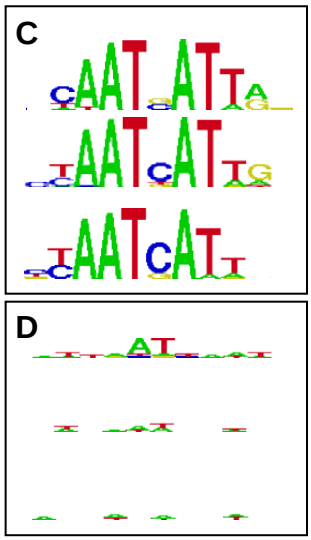

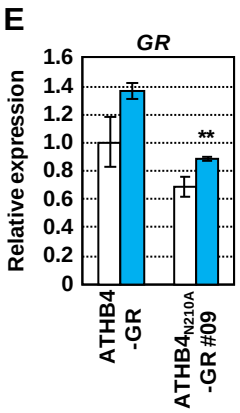

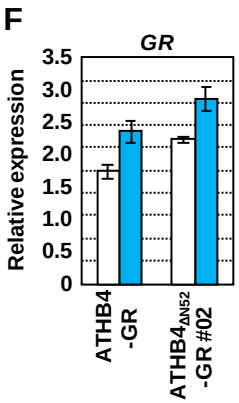

Fig. S8 Detection of GFP-fused proteins in two transgenic ATHB4 derivative lines. **(A)** GFP levels were assayed in extracts from 35S:ATHB4-GFP and 35S:0HZC-GFP seedlings grown under W for 7 days and then either kept under W or W+FR for 4 hours. **(B)** Tubulin (TUB) levels were assayed in the same blot after stripping the membrane as a loading control. Bands were detected by immunoblot using commercial antibodies against GFP (antiGFP, panel **A**) or TUB (antiTUB, panel **B**).

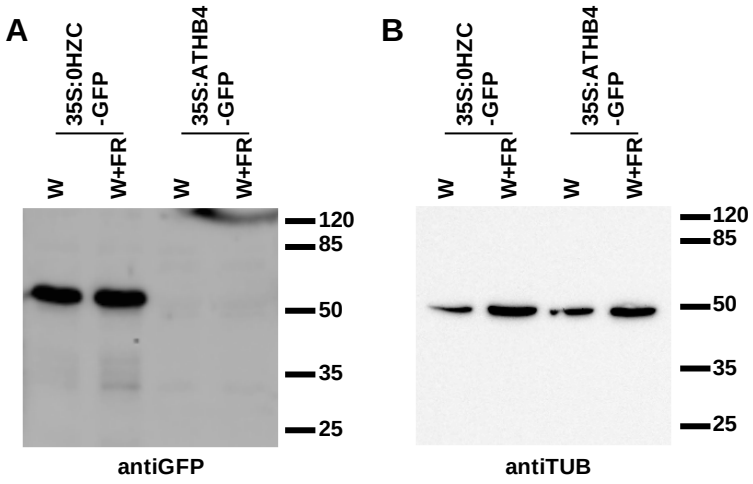

Fig. S9 ATHB4 promotes upwards leaf curling. **(A)** Effect of *ATHB4-GFP* overexpression on leaf polarity. Rosettes (upper part), and the adaxial (ad) and abaxial (ab) views of a leaf (lower part) are shown. A representation of a leaf transversal section is shown to the right of the leaf pictures. Wild-type (Col-0) and 35S:ATHB4-GFP plants were germinated and grown for 20 days in short day conditions (8 h light / 16 h of dark). Scale bars = 1 cm. **(B)** Cartoon describing the growth conditions employed to analyze the leaf phenotypes in the inducible lines. Wild-type and 35S:ATHB4-GR plants were grown under short day conditions. On day 20 after germination, plants were either mock-treated (-DEX) or DEX-treated (+DEX) by adding a drop of 10 µl in the apical meristem of 2.5 % (v/v) ethanol, 0.05 % (v/v) Tween 20 (-DEX) or 5 µM DEX in the same solution, respectively. During a total of 10 days, plants were treated 7 days with these solutions around the same time. **(C)** Effect of ATHB4 induced-activity on leaf polarity shown in leaves (adaxial view in the left, abaxial view on the middle and transverse representation on the right) treated as indicated in **B**. Adaxial (ad, upper part) and abaxial views (ab, middle part), and representation of leaf transversal sections (lower part) are shown. Leaves pictures are shown to the same scale. Scale bar = 1 cm.

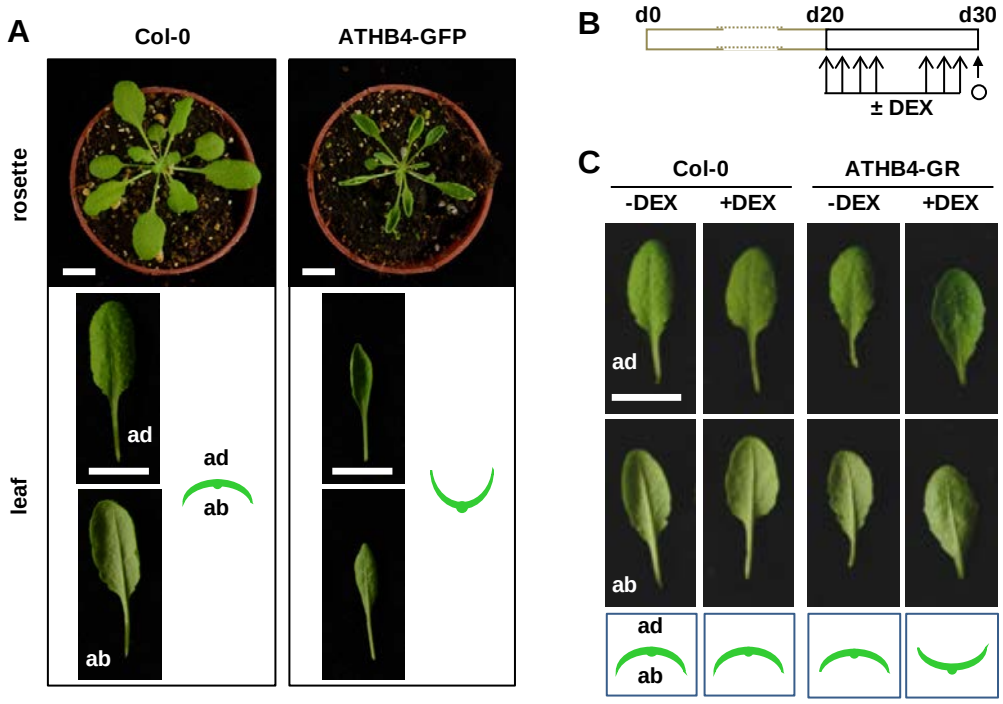

Table S1 Primers used for amplifying and cloning genes used in this work. ([1]) MCS, Multiple cloning site for the preparation of pMS51.

Gene name	**Name, oligonucleotide sequences (5'→3')**
GR	BO70, GGA-TCT-AGA-ATG-GGC-GAG-CTC-CCA-GAA-GCT-CG
	BO71, CCT-ACT-AGT-TTT-TTG-ATG-AAA-CAG-AAG-CTT-TTT-G
ATHB4	CSO7, GGG-GAT-CCG-CGA-CCT-GAT-TTT-TGC-TG
	JO284, AGG-ACA-ATG-GGG-GAA-AGA-GAT
	MSO12, GAA-TTC-ATG-CGC-GGA-GGG-GGA-AGC
	MGO1, CGA-TGC-GCG-GAG-GGG-GAA-GCG-GTG
	MGO2, CGA-TGA-CGG-AGG-TTG-ATT-GTG-AG
	MGO20, GAA-GTG-TGG-TTT-CAG-GCC-CGT-AGG-GCA-AGG-ACG-AAG
	MGO21, CCT-TGC-CCT-ACG-GGC-CTG-AAA-CCA-CAC-TTC-AAC
	MGO22, GAT-TCA-TAA-CAT-CTC-TGC-GAC-TCA-TCT-GTT-TCA-ATC-TTC-TGG
	MGO23, GAA-ACA-GAT-GAG-TCG-CAG-AGA-TGT-TAT-GAA-TCT-TTG-G
	MGO3, GGG-GAT-CCA-GTC-ATG-TGC-ATG-TAG-AG
	MGO4, GGG-GAT-CCT-TGT-TTC-AGC-TTC-GTC-CTT-GC
	MGO50, CGA-TGC-AGA-AGA-TTC-ATA-ACA-TCT-CTT-GG
	MGO51, GGG-GAT-CCT-GAG-CAA-GAA-GCT-CTC-TCC-GC
	MSO36, GAT-GGG-TTG-GGT-GCG-AGT-CTA-AGC-TTG-GGA-AAT-AGT-C
	MSO37, CAA-GCT-TAG-ACT-CGC-ACC-CAA-CCC-ATC-ATC-TCT-TTC
HAT1	CSO9, ATC-ATG-ATG-ATG-GGT-AAA-GAG-GAT-TTG
	CSO10, AAG-TTA-AGA-CCT-AGG-ACG-CAT-CAC-ATC
HAT2	RO3, AAC-ATG-ATG-ATG-GGC-AAA-GAA-G
	CSO8, GGG-GAT-CCC-GAT-CGT-GGA-CGC-AAG-GC
MCS[1]	MSO44, CAT-GGC-GTC-GAC-AAG-ATC-TGC-CA
	MSO45, CTA-GTG-GCA-GAT-CTT-GTC-GAC-GC
TPL	MJO11, GGG-GAC-AAG-TTT-GTA-CAA-AAA-AGC-AGG-CTT-CAT-GTC-TTC-TCT-TAG-TAG-AGA-GCT-C
	MJO13, GGG-GAC-CAC-TTT-GTA-CAA-GAA-AGC-TGG-GTC-CGT-TGG-TTG-AAA-TGG-CCC-GTG

Table S2 Primers used for qPCR analyses. Primers for transcript level analyses by RT-qPCR of *HAT2*, *SAUR15* and *UBQ10* were described elsewhere (Sorin *et al.*, 2009; Galstyan *et al.*, 2011; Cifuentes-Esquivel *et al.*, 2013; Gallemi *et al.*, 2016). Primers for ChIP analyses of *ATHB2* were described previously (Brandt *et al.*, 2012).CDS, coding sequence; Pro, Promoter region.

Gene name - genome location (use - code in Fig 6)	**Name, oligonucleotide sequences (5'→3')**
GR (RT-qPCR)	MGO42, TTC-AGC-AAG-CCA-CTG-CAG-G
	MGO43, GCT-GTG-GTA-ATG-CTG-CAG-GAA
UBQ10 - CDS (RT-qPCR, ChIP -U1)	BO40, AAA-TCT-CGT-CTC-TGT-TAT-GCT-TAA-GAA-G
	BO41, TTT-TAC-ATG-AAA-CGA-AAC-ATT-GAA-CTT
ATHB2 - Pro (ChIP - A1)	MGO55, GTC-CGT-CGA-TGT-CCT-CCT-AA
	MGO56, AAT-AAC-GAC-GAC-GCC-AAA-AG
ATHB2 - Pro (ChIP - A2)	MGO57, TAT-CGT-CGG-GCT-ACA-AAA-CC
	MGO58, CAC-ACT-GCT-GCC-GTA-CAC-TT
ATHB2 - Pro (ChIP - A3)	MGO59, GGA-TGT-GCA-ATT-GTT-CAT-GGT
	MGO60, TGG-TTA-GAT-CGT-TGA-GTC-GTG
ATHB2 - CDS (RT-qPCR, ChIP - A4)	MGO26, GGA-GGT-AGA-CTG-CGA-GTT-CTT-ACG
	MGO27, TGC-ATG-TAG-AAC-TGA-GGA-GAG-AGC
HAT2 - Pro (ChIP - H1)	MGL9, AAT-TGT-CCT-CTC-ACA-TGT-ACT-G
	MGL10, GTG-ATG-CAA-ACC-TCA-AAT-TC
HAT2 - Pro (ChIP - H2)	MGL7, CTG-ACC-AAG-TGC-GTT-ATA-TC
	MGL8, ATC-ATG-CTT-TGC-GGA-CTC-TC
HAT2 - Pro (ChIP - H3)	MGL5, GCA-TGT-GGG-TCA-TAA-CAG
	MGL6, GTA-GGC-AGC-AGT-TAA-AGG

Table S3 Overlap of bioset of DEX-regulated genes in –CHX and +CHX treated 35S:ATHB4-GR (pCS19) seedlings, BH<0.05, FC≥1.5 (104 genes: 7 up-regulated (first seven genes of the list); + 97 down-regulated). Location of a 9-mer ATHB4 binding site is indicated when found within the 3000 bp upstream the transcriptional start.

AGI #	Sequence Description	ATHB4-binding site location
At2g35880	TPX2 (targeting protein for Xklp2) protein family	
At3g20340	Expression of the gene is downregulated in the presence of paraquat, an inducer of photoxidative stress	(-1895) TAATGATTG
At3g28220	TRAF-like family protein	
At3g28270	Protein of unknown function (DUF677)	(-656) TAATTATTG
At5g20790	Unknown protein	
At5g24150	SQUALENE MONOOXYGENASE 5 (SQE5)	(-2350) TAATCATTA
At5g52310	LOW-TEMPERATURE-INDUCED 78 (LTI78)	
At1g06160	OCTADECANOID-RESPONSIVE ARABIDOPSIS AP2/ERF 59 (ORA59)	(-1201) TAATCATTA
At1g07440	NAD(P)-binding Rossmann-fold superfamily protein	(-15) CAATGATTG
At1g11350	S-DOMAIN-1 13 (SD1-13)	
At1g14540	PEROXIDASE 4 (PER4)	(-1210) TAATTATTG
At1g21250	CELL WALL-ASSOCIATED KINASE (WAK1)	
At1g22570	Major facilitator superfamily protein	
At1g23090	SULFATE TRANSPORTER 91 (AST91)	
At1g25560	TEMPRANILLO 1 (TEM1)	(-1885) TAATTATTG
At1g29050	TRICHOME BIREFRINGENCE-LIKE 38 (TBL38)	(-538) TAATCATTG
At1g29430	SAUR-like auxin-responsive protein family	
At1g29440	SMALL AUXIN UP RNA 63 (SAUR63)	
At1g29500	SAUR-like auxin-responsive protein family	
At1g29510	SMALL AUXIN UPREGULATED 68 (SAUR68)	
At1g33790	Jacalin lectin family protein	
At1g33960	AVRRPT2-INDUCED GENE 1 (AIG1)	
At1g51805	Leucine-rich repeat protein kinase family protein	(-1840) TAATCATTG; (-804) CAATGATTG
At1g51890	Leucine-rich repeat protein kinase family protein	
At1g55760	BTB/POZ domain-containing protein	
At1g66940	Protein kinase-related	(-2547) TAATCATTA; (-381) TAATCATTA
At1g68500	Unknown protein	(-554) TAATTATTG
At1g68520	B-box type zinc finger protein with CCT domain	(-590) TAATGATTA
At1g70690	HOPW1-1-INDUCED GENE1 (HWI1)	

At1g72450	JASMONATE-ZIM-DOMAIN PROTEIN 6 (JAZ6)	
At1g73830	BR ENHANCED EXPRESSION 3 (BEE3)	
At1g77210	SUGAR TRANSPORT PROTEIN 14 (STP14)	
At1g78450	SOUL heme-binding family protein	
At2g02010	GLUTAMATE DECARBOXYLASE 4 (GAD4)	(-1251) TAATTATTG
At2g05520	GLYCINE-RICH PROTEIN 3 (GRP-3)	
At2g06850	XYLOGLUCAN ENDOTRANSGLUCOSYLASE/HYDROLASE 4 (XTH4)	
At2g19190	FLG22-INDUCED RECEPTOR-LIKE KINASE 1 (FRK1)	
At2g21650	A member of a small sub-family of single MYB transcription factors (MATERNAL EFFECT EMBRYO ARREST 3, MEE3).	
At2g29740	UDP-GLUCOSYL TRANSFERASE 71C2 (UGT71C2)	
At2g30010	TRICHOME BIREFRINGENCE-LIKE 45 (TBL45)	
At2g31730	Basic helix-loop-helix (bHLH) DNA-binding superfamily protein	
At2g32210	Unknown protein	(-431) TAATTATTG
At2g36950	Heavy metal transport/detoxification superfamily protein	
At2g38310	PYR1-LIKE 4 (PYL4)	
At2g40330	PYR1-LIKE 6 (PYL6)	
At2g43140	bHLH DNA-binding superfamily protein, BHLH129	
At2g43570	"chitinase, putative" (CHI)	(-1948) TAATGATTG; (-1850) TAATTATTG
At2g43590	Chitinase family protein	(-288) CAATCATTG
At2g43820	UDP-GLUCOSYLTRANSFERASE 74F2 (UGT74F2)	(-1073) AATGATTG; (-990) TAATGATTG
At2g44380	Cysteine/Histidine-rich C1 domain family protein	(-2353) TAATCATTG
At2g46450	CYCLIC NUCLEOTIDE-GATED CHANNEL 12 (CNGC12)	(-113) TAATCATTA
At3g02240	ROOT MERISTEM GROWTH FACTOR 7 (RGF7)	
At3g06070	unknown protein	
At3g13760	Cysteine/Histidine-rich C1 domain family protein	
At3g13980	unknown protein	(-105) TAATCATTG
At3g14225	GDSL-MOTIF LIPASE 4 (GLIP4)	
At3g16240	DELTA TONOPLAST INTEGRAL PROTEIN (DELTA-TIP)	
At3g16360	HPT PHOSPHOTRANSMITTER 4 (AHP4)	
At3g22231	PATHOGEN AND CIRCADIAN CONTROLLED 1 (PCC1)	
At3g23550	MATE efflux family protein	
At3g47960	Major facilitator superfamily protein	
At3g48740	Encodes a member of the SWEET sucrose efflux transporter family proteins (SWEET11)	(-2269) TAATGATTG; (1748) TAATGATTG; (-1766) TAATTATTG
At3g49620	DARK INDUCIBLE 11 (DIN11)	
At3g61460	BRASSINOSTEROID-RESPONSIVE RING-H2 (BRH1)	(-2482) CAATGATTG

At3g62630	Protein of unknown function (DUF1645)	
At4g03510	RING MEMBRANE-ANCHOR 1 (RMA1)	
At4g04220	RECEPTOR LIKE PROTEIN 46 (RLP46)	
At4g08290	Nodulin MtN21-like transporter family protein	
At4g11460	CYSTEINE-RICH RLK (RECEPTOR-LIKE PROTEIN KINASE) 30 (CRK30)	
At4g15920	Nodulin MtN3 family protein (SWEET17)	
At4g17460	HAT1	(-1567) TAATGATTA; (-883) CAATGATTG
At4g17500	ETHYLENE RESPONSIVE ELEMENT BINDING FACTOR 1 (ERF-1)	
At4g17870	PYRABACTIN RESISTANCE 1 (PYR1)	
At4g19820	Glycosyl hydrolase family protein with chitinase insertion domain	
At4g21410	CYSTEINE-RICH RLK (RECEPTOR-LIKE PROTEIN KINASE) 29 (CRK29)	
At4g23210	Encodes a Cysteine-rich receptor-like kinase (CRK13)	
At4g31800	WRKY DNA-BINDING PROTEIN 18 (WRKY18)	
At4g31970	"CYTOCHROME P450, FAMILY 82, SUBFAMILY C, POLYPEPTIDE 2" (CYP82C2)	(-2027) TAATTATTG
At4g37790	HAT22	
At4g38840	SAUR-like auxin-responsive protein family	(-2560) TAATCATTG; (-1360) TAATTATTG
At4g38850	SMALL AUXIN UPREGULATED 15 (SAUR15)	
At5g01740	Nuclear transport factor 2 (NTF2) family protein	(-2811) TAATTATTG; (-897) TAATGATTG
At5g02760	Protein phosphatase 2C family protein	
At5g04230	PHENYL ALANINE AMMONIA-LYASE 3 (PAL3)	(-947) TAATTATTG
At5g07460	PEPTIDEMETHIONINE SULFOXIDE REDUCTASE 2 (PMSR2)	(-570) TAATCATTG
At5g07580	encodes a member of the ERF (ethylene response factor) subfamily B-3 of ERF/AP2 transcription factor family	(-295) TAATTATTG
At5g10030	Encodes TGACG MOTIF-BINDING FACTOR 4 (TGA4), a member of basic leucine zipper transcription gene family	
At5g14120	Major facilitator superfamily protein	(-2295) CAATGATTG
At5g15830	BASIC LEUCINE-ZIPPER 3 (bZIP3)	(-1995) TAATGATTG; (-1172) TAATTATTG
At5g17860	CALCIUM EXCHANGER 7 (CAX7)	
At5g20250	DARK INDUCIBLE 10 (DIN10). Encodes a member of glycosyl hydrolase family 36	
At5g21105	Plant L-ascorbate oxidase	(-1323) TAATTATTG
At5g24210	alpha/beta-Hydrolases superfamily protein	
At5g38900	Thioredoxin superfamily protein	
At5g43170	Encodes ZINC-FINGER PROTEIN 3 (ZF3)	(-356) TAATGATTG

At5g43890	YUCCA5 (YUC5)	
At5g47370	HAT2	(-2930) TAATCATTG
At5g55930	OLIGOPEPTIDE TRANSPORTER 1 (OPT1)	
At5g59080	putative protein	(-1155) TAATTATTG
At5g61520	monosaccharide transporter STP3	
At5g61590	encodes a member of the ERF subfamily B-3 of ERF/AP2 transcription factor family	
At5g61600	ETHYLENE RESPONSE FACTOR 104 (ERF104)	
At5g64770	ROOT MERISTEM GROWTH FACTOR 9 (RGF9)	
At5g64780	putative protein similar to unknown protein (pir||T04031)	

Table S4 ATHB4-interacting proteins identified in the Y2H screen. ([1]) A Predicted Biological Score (PBS) is computed to assess the interaction reliability for each interaction. This score represents the probability of an interaction to be non-specific: it is an e-value, primarily based on the comparison between the number of independent prey fragments found for an interaction and the chance of finding them at random (background noise). The value varies between 0 and 1. Several thresholds have been arbitrarily defined in order to rank the results in 5 categories from A (the highest confidence rank) to D. ([2]) The Selected Interaction Domain (SID) is the amino acid sequence shared by all prey fragments matching the same reference protein. SIDs have been found in numerous cases to correspond to an identified structural or functional domain.

Name (AGI code)	**PBS[1] (clone number)**	**Main characteristics**	**SID[2] (total residues)**	**Identified domain/motif within SID**
HAT2 (At5g47370)	A (17)	DNA-binding, transcription factor	95-283 (283)	HD-Zip
HAT22 (At4g37790)	D (3)	DNA-binding, transcription factor	41-248 (278)	HD-Zip
HAT3 (At3g60390)	C (3)	DNA-binding, transcription factor	136-315 (315)	HD-Zip
HAT9 (At2g22800)	D (1)	DNA-binding, transcription factor	86-274 (274)	HD-Zip
TPL (At1g15750)	A (8)	Transcriptional co-repressors	1-193 (1131)	LisH dimerization motif
TPR4 (At3g15880)	C (5)	Transcriptional co-repressors	30-164 (1135)	LisH dimerization motif

Methods S1 Generation of GFP- and GR-fused constructs for plant transformation.

Truncated DNA fragments of *ATHB4* were PCR-amplified with specific primers using as DNA template pCS19, a plasmid containing *ATHB4* full-length sequence described elsewhere (Sorin *et al.*, 2009). The specific primer combinations (Table S1) were: JO284+MGO3 (NHZ0), MGO1+MGO3 (0HZ0), MGO2+MGO3 (00Z0), MGO2+CSO7 (00ZC), MGO2+CSO7 (0HZC), JO284+MGO4 (NH00), MGO1+MGO4 (0H00) and MGO50+CSO7 ($ATHB4_{\Delta N52}$). The resulting PCR fragments were cloned in pCRII-TOPO (Invitrogen) to give a series of constructs named as pMG16 (NHZ0), pMG17 (0HZ0), pMG18 (00Z0), pMG19 (00ZC), pMG20 (0HZC), pMG21 (NH00), pMG22 (0H00) and pMG42 ($ATHB4_{\Delta N52}$). Inserts were sequenced to confirm their identity. The mutated derivative $ATHB4_{N210A}$ was generated by double PCR-based site-directed mutagenesis. First specific mutated primers (MGO20 and MGO21) were used to amplify a fragment with the point mutation: MGO20 with CSO7 and JO284 with MGO21 for $ATHB4_{N210A}$. Those mutated PCR fragments were used for a full-length amplification with JO284 and CSO7 primers. The final insert was cloned into pCRII-TOPO vector and named as pMG35 ($ATHB4_{N210A}$). Insert was sequenced to confirm its identity.

To generate a plasmid to overexpress the full-length ATHB4 fused to the *GFP*, an *Spe*I-*Xba*I fragment of pCS12, which contains *ATHB4* ORF with the stop codon removed (Sorin *et al.*, 2009), was subcloned into the *Spe*I site of the binary vector pCAMBIA1302 (www.cambia.org) to generate pBJ3 (35S:ATHB4-GFP). For the ATHB4-truncated GFP fusions, we first generated a pCAMBIA1302-derivative vector with a modified multiple cloning site. Briefly, annealed MSO44 and MSO45 oligos, which produce a short dsDNA flanked by *Nco*I-*Spe*I restriction sites, were inserted into pCAMBIA1302 digested with the same restriction enzymes, resulting in vector pMS51. The *Bam*HI fragments from the pCRII-TOPO-derived vectors pMG16-22 were cloned in frame with the *GFP* tag in pMS51 digested with *Bgl*II, resulting in pMS52 (35S:NHZ0-GFP), pMS53 (35S:0HZ0-GFP), pMS54 (35S:00Z0-GFP), pMS55 (35S:00ZC-GFP), pMS56 (35S:0HZC-GFP), pMS57 (35S:NH00-GFP) and pMS58 (35S:0H00-GFP). For biolistic experiments, plasmid was purified using a commercial kit (Qiagen Plasmid Midi kit, http://www.qiagen.com) following manufacturer's protocol.

For the GR fusions, we first generated pMG15, a binary vector with the 35S promoter and the *GR*+OCS terminator separated by a convenient multiple cloning site (35S:-GR). Briefly, the *GR*-containing fragment obtained after digesting pGREEN0029 vector (Hellens *et al.*, 2000) with *Sal*I+Klenow (blunt-ended) and *Bam*HI was cloned in pCS14 (Sorin *et al.*, 2009) digested with *Eco*RI+Klenow and *Bam*HI to give pMG15. *Bam*HI fragments from the pCRII-TOPO-derived vectors pMG16-22, pMG35 and pMG42 were inserted in frame with the GR domain in the vector pMG15 also digested with *Bam*HI, generating pMG23 (35S:NHZ0-GR), pMG24 (35S:0HZ0-GR), pMG25 (35S:00Z0-GR), pMG26 (35S:00ZC-GR), pMG27 (35S:0HZC-GR), pMG28 (35S:NH00-GR), pMG29 (35S:0H00-GR), pMG60 (35S:N000-GR), pMG37 (35S:ATHB4$_{N210A}$-GR) and pMG44 (35S: ATHB4 $_{\Delta N52}$-GR).

To generate a binary plasmid to overexpress the full-length *HAT1*, the whole coding sequence was amplified using specific primers (CSO9+CSO10) a cDNA as a template. The corresponding PCR fragments were subcloned in pCRII-TOPO (Invitrogen) to give pCS30. The insert was sequenced and no mutations were found in the coding region. The plasmid was digested with *Eco*RI, blunt-ended with Klenow, and cloned in the binary vector pBinAr (Höfgen & Willmitzer, 1990) digested with *Sma*I to give pCS31 (35S:HAT1).

To generate a binary plasmid to overexpress the full-length *HAT2* fused to the *GR*, *HAT2* sequence was amplified without the stop codon using specific primers (RO3 + CSO8, which introduces a *Bam*HI site) using cDNA as a template. The corresponding PCR fragments were subcloned in pCRII-TOPO (Invitrogen) to give pCS8. The insert was sequenced and no additional mutations were found in the coding region. pCS8 was digested with *Xba*I and *Bam*HI and cloned in frame with the GR domain in the vector (Hellens *et al.*, 2000) digested with the same restriction enzymes to give pCS9 (HAT2-GR). The pPZP-Hd1(SG) vector, a plasmid derived from the pPZP2Ha3(-) (Fuse *et al.*, 2001), was digested with *Hind*III and religated, which removed the Hd1(SG) gene from rice, resulting into pJF277 (this binary vector contains the 35S promoter, a multiple cloning site and the Nos terminator cassette, and confers hygromycin resistance to transgenic plants). The *Eco*RI fragment from pCS9 was blunt-ended with Klenow and subcloned into pJF277 digested with *Not*I and blunt-ended, generating pCS10 (35S:HAT2-GR).

These binary vectors were introduced in *Agrobacterium tumefaciens* $C_{58}C_1$ (pGV2260) by electroporation, and transformed colonies were selected in YEB media supplemented with Rifampicin (100 µg/mL), Kanamycin (25 µg/mL) and Ampicillin (100 µg/mL). Arabidopsis plants (Col-0) were transformed by floral dipping and transgenic seedlings were selected. Transgene presence in T_1 plants was verified by PCR analysis using specific primers on plant genomic DNA isolated from young leaves. Only lines with a single T-DNA insertion (as estimated from the segregation of the marker gene in T_2 populations) were eventually selected, as described before (Roig-Villanova *et al.*, 2006).

Methods S2 Transcriptomic analyses.

For microarray analysis, 35S:ATHB4-GR (pCS19) seedlings were grown for 7 days on filter paper placed on top of GM- medium plates at 22°C under continuous white light (W, 25 µmol m^{-2} s^{-1} of photosynthetically active radiation). Seedlings were transferred to new plates containing 4 ml of water supplemented or not with 5 µM DEX and/or 50 µM CHX (which resulted in a total of 4 treatments). Triplicate samples were harvested individually 4 h after beginning the DEX/CHX treatment (a total of 12 samples). RNA was extracted using the plant RNeasy extraction kit (Qiagen), and over 1 mg of RNA from each sample was sent to the NASC Affy Gene ChIP service, who performed an ATH1 Genome Array. The full data set is available to download from the NASCarrays database (http://affymetrix.Arabidopsis.info/; reference: FTP:NASCARRAY545). Microarray data were analyzed as indicated (Kaufmann *et al.*, 2010). Briefly, data were imported into the Resolver gene expression data analysis system version 7.1 (Rosetta Biosoftware, http://www.ceibasolutions.com/rosetta-about) and processed as described (Wellmer *et al.*, 2006). Resolver uses a platform-specific error model-based approach to stabilize the variance estimation to improve the specificity and sensitivity in differential gene expression detection (Weng *et al.*, 2006). Data from the biological replicates of each condition were combined, resulting in an error-model weighted average of the replicates. The Pvalues for differential expression calculated by Resolver were adjusted for multi-hypothesis testing using the Benjamini & Hochberg procedure, as implemented in the Bioconductor multtest package in R (http://www.bioconductor.org/packages/bioc/stable/src/contrib/html/multtest.html). Genes

for which the Benjamini & Hochberg-adjusted P-value (BH) was <0.05 and an absolute fold-change (FC) cutoff of 1.5 were considered differentially expressed in response to 4 h of DEX treatment. These thresholds resulted in the identification of a total of 433 (-CHX), and 1055 (+CHX) genes that showed expression changes (FC>1.5) after 4 h of initiating the DEX treatment in pCS19 seedlings (Table S3). The overlap of these subsets of DEX-regulated genes resulted in the identification of a total of 104 genes that showed transcriptional changes regulated directly by ATHB4 activity. Among these genes, several well-described HD-Zip members, such as HAT1, HAT2, and HAT22, were found.

Methods S3 Gene expression analysis by RNA blot analysis.

Total RNA was isolated from seedlings, electrophoresed and blotted as described (Roig-Villanova *et al.*, 2006). The probe for analyzing *GR* expression was generated amplifying pGREEN0029 plasmid with BO70+BO71 primers. 25S rRNA signal (Roig-Villanova *et al.*, 2006) was used as a loading control. Probe labeling, and membrane hybridization, washes, exposure and quantification of radioactive signal were carried out as described (Martinez-Garcia *et al.*, 2002). These experiments were conducted at least twice.

Methods S4 Yeast Two Hybrid (Y2H) assays.

Generation of constructs for Y2H assays

The HD-Zip domain of ATHB4 (0HZ0) was PCR-amplified with MSO12 and MGO3, using as DNA template pCS19. The resulting PCR fragment was cloned in pCRII-TOPO to give pMS35 (0HZ0). Insert was sequenced to confirm its identity. An *Eco*RI-*Bam*HI fragment of pMS35, which contains the HD-Zip domain of ATHB4 (0HZ0), was subcloned into the same sites of pGBKT7 and pGADT7 vectors, resulting in pMS39 (BD-0HZ0) and pMS37 (AD-0HZ0), respectively.

The N-terminal part of ATHB4 (N000) was inserted into the entry vector pENTR-3C (Invitrogen) for further cloning employing the Gateway system. To do so, the *Eco*RI fragment of pMG17 (containing the truncated N000 fragment) was subcloned into the same site of pENTR-3C, resulting in pMJ32. The N-terminal part of ATHB4 was subcloned in frame with the DNA-binding domain (BD) and transcription activation domain (AD) of the yeast GAL4 protein after a LR

clonase reaction (Invitrogen) between pMJ32 and the destination vectors pGBKT7gateway (pGBKT7-GW) and pGADT7-GW (Chini *et al.*, 2009), resulting in pMJ38 (BD-N000) and pMJ39 (AD-N000).

The N-terminal part of TOPLESS (NtTPL, first 242 amino acids) was subcloned by PCR with specific primers, MJO11+MJO13, using as a template pENTR-TPL, a gateway vector containing the full length TPL sequence (Graeff *et al.*, 2016). The resulting PCR fragment was cloned in the pDONR207 vector (Clontech) after a BP clonase reaction (Invitrogen), giving pMJ16 (NtTPL). The insert was sequenced to confirm its identity. The NtTPL fragment was subcloned in frame with the BD and AD after a LR clonase reaction (Invitrogen) between pMJ16 and pGBKT7-GW and pGADT7-GW (Chini *et al.*, 2009), respectively, resulting in pMJ22 (BD-NtTPL) and pMJ23 (AD-NtTPL).

Y2H screening

Yeast two-hybrid screening was performed by Hybrigenics S.A., Paris, France (http://www.hybrigenics-services.com). The full-length sequence of ATHB4 was PCR amplified and cloned into pB27 as a C-terminal fusion to LexA (N-LexA-ATHB4-C). The construct was checked by sequencing the entire insert and used as a bait to screen a random-primed Arabidopsis seedlings cDNA library constructed into pP6. Details of the employed library for the screening are provided elsewhere (Cifuentes-Esquivel *et al.*, 2013). 63.9 million clones (about 6 -fold the complexity of the library) were screened using a mating approach with Y187 (mat α) and L40ΔGal4 (mat a) yeast strains as previously described (Fromont-Racine et al., 1997). 291 His+ colonies were selected on a medium lacking Trp, Leu and His, and supplemented with 1.0 mM 3-aminotriazole to handle bait autoactivation. The prey fragments of the positive clones were amplified by PCR and sequenced at their 5’ and 3’ junctions. The resulting sequences were used to identify the corresponding interacting proteins in the GenBank database (NCBI) using a fully automated procedure. A confidence score (PBS, for Predicted Biological Score) was attributed to each interaction as previously described (Formstecher *et al.*, 2005).

Y2H directed assays

To perform directed Y2H growth assays we employed two different systems: co-transformation (Figure S2B-C) and cell mating (Figure 6A). Yeast cells of the AH109 strain were co-transformed

with the different pairs of BD/AD constructs. Independent transformants were selected on synthetic medium (SD) lacking Leu and Trp (SD-LW), and colonies subsequently transferred to SD lacking Ade, His, Leu and Trp (SD-AHLW) to test for protein-protein interaction. Co-transformations were repeated at least twice with identical results. For mating, yeast cells of the leucine auxotroph YM4271a strain were transformed with the AD derivative constructs, whereas the tryptophan auxotroph pJ694α strain was transformed with the BD derivative constructs. Selected independent colonies on SD lacking either Leu (SD-L) (AD) or Trp (SD-W) (BD) were grown in liquid medium, and then allowed to mate by mixing equal volumes of the two types of transformed yeast cells. Mated cells were selected on SD-LW plates and then transferred to SD-HLW plates to test for protein-protein interaction. Co-transformations or mating experiments were repeated at least twice with identical results. Different dilutions were use for testing the interactions.

Methods S5 Subcellular localization analyses.

Generation of constructs for BiFC analyses

The full-length TPL sequence present in pENTR-TPL (Graeff *et al.*, 2016) was recombined into the pYFN43 gateway destination vector (Belda-Palazon *et al.*, 2014) resulting in pMJ27 (35S:YN-TPL).

The *Eco*RI fragment of pCS12 (containing full-length ATHB4 cDNA) was subcloned into the same site of the gateway vector pENTR3C, which resulted in the pMJ29 plasmid (it conferred kanamycin resistance in bacteria). Next, we performed a LR clonase reaction (Invitrogen) combining pMJ29 and the gateway vector for yeast pGADT7-GW (carbenicillin resistance) giving pMJ33. The resulting pMJ33 was cloned in the pDONR207 vector (Clontech) after a BP clonase reverse reaction (Invitrogen), giving pMJ34 (gentamycin resistance). Finally, an LR clonase reaction between pMJ34 and the destination vector pYFC43 (Belda-Palazon *et al.*, 2014) resulted in pMJ36 (35S:YC-ATHB4).

Subcellular localization analyses: microbombardments of onion epidermal cells and agroinfiltration of *Nicotinana benthamiana* leaves

Onion epidermal cells were bombarded using a Biolistic PDS1000/He system (Bio-Rad) according to the manufacturer's protocol. After bombardment, cells were recovered on plates of 1xGM– supplemented with 1% (w/v) sucrose for 12-18 h at 22ºC in the dark.

BiFC to validate the interaction between YN-TPL (pMJ27) and YC-ATHB4 (pMJ36) was performed by transient expression in *Nicotiana benthamiana* plants (tobacco). Briefly, a colony of *Agrobacterium tumefaciens* (strain GV3101) transformed with either pMJ27 or pMJ36 was inoculated in 3 mL of YEB with appropriate antibiotics (100 $\mu g \cdot mL^{-1}$ Rifampicin, 25 $\mu g \cdot mL^{-1}$ gentamicin, 25 $\mu g \cdot mL^{-1}$ kanamycin) and grown overnight at 28ºC. One mL of the overnight culture was inoculated in 25 mL of YEB (supplemented with the indicated antibiotics) and grown overnight at the same temperature. After measuring the OD_{600} of the grown culture, cells were sedimented (5000g for 15 min) and the pellet was resuspended in Resuspension Solution (Li, 2011) to get a final OD_{600} of 1.0. Cell resuspension was incubated for 2 hours at room temperature before doing the leaf infiltration with a 1 mL syringe. Plants were returned to the growing chamber and after 3 days fluorescence was observed by confocal microscopy. The fluorescence was detected using a Leica SP5 II (www.leica.com) or an Olympus FV 1000 (www.olympus.com/) confocal microscope. Images were processed with the LAS AF Lite and Olympus FV software, respectively. After excitation by an Ar 488 nm laser, GFP was visualized with a band-pass 500–545 nm filter. The Red Fluorescent Protein (dsRed) was visualized using excitation of He/Ne 543 nm and a 555-700 nm filter.

Methods S6 Expression of recombinant ATHB4-MBP for Protein Binding Microarrays (PBMs). The *Eco*RI fragment from pCS12, containing the full-length ATHB4 cDNA, was subcloned in the vector pMAL-c2x digested with the same enzyme to give pMG46. Similarly, the *Eco*RI fragment from pMG35, containing the mutated $ATHB4_{N210A}$ cDNA, was subcloned in the vector pMAL-c2x digested with the same enzyme to give pMG64. These pMAL-c2x-derived vectors allow producing the fusion proteins ATHB4-MBP and $ATHB4_{N210A}$-MBP. *Escherichia coli* (strain BL-21 with the plasmid pGROE) was transformed with pMG46 and pMG64, and the recombinant

proteins were expressed in liquid cultures after 4h induction with IPTG. The resulting 50 mL cell pellets were then purified and used for the PBM as described elsewhere (Godoy *et al.*, 2011).

Methods S7 Chromatin immunoprecipitation (ChIP).

For preparing chromatin extracts, Arabidopsis seedlings were grown on nylon mesh placed on top of 0.5xGM– for 7 days under W (6 plates, ca. 100 seedlings per plate). About 0.5 g of seedlings was harvested per sample. Chromatin immunoprecipitation was performed as described in http://www.abcam.com, with the following minor modifications: chromatin was extracted in 100 µl of cold nuclei lysis buffer and sonicated for 10 min at 4°C with sonicator Bioruptor® (Diagenode) set to "HIGH" (30 sec "ON cycle", 30 sec "OFF cycle"). Samples were immunoprecipitated with 1 µg of anti-GFP (A-11122, Thermo Fisher Scientific, US).

Methods S8 Protein extraction and immunoblot analyses.

For preparing protein extracts, around 60 seedlings grown under W for seven days (about 70-80 mg of fresh weight) of each genotype were harvested and frozen in liquid nitrogen until processed. Plant material was ground before Extraction Buffer (EB) (40 mM Tris-HCL pH 6.8, 4% (w/v) SDS, 5% glycerol, 1x proteases inhibitor cocktail - Cat. No. 11873580001, Roche; www.sigmaaldrich.com) was added (1µl of EB per mg fresh weight). The extract was kept at room temperature to avoid SDS precipitation. Samples were centrifuged at 14000 *g*, 3 min at room temperature and the supernatant was recovered. The protein concentration was determined using the Pierce BCA Protein Assay Kit (Cat. No. 23225; www.thermofisher.com). Electrophoresis and immunoblotting were carried as described (Martinez-Garcia *et al.*, 2014) with the following modifications: a 10% SDS-PAGE gel was prepared to resolve our proteins of interest; a 50 µg protein aliquot of each sample was loaded per lane; immunoblot was carried out in TBST buffer (20 mM Tris pH 7.5, 150 mM NaCl, 0.05 % Tween 20) containing 0.5 % (w/v) milk protein with a 1:1000 dilution of rabbit polyclonal anti-GFP (Cat. No. A11122, https://www.thermofisher.com) as primary antibody; membranes were stripped and rehybridized with a commercial mouse mAb against α-tubulin (Cat. No. T6074; www.sigmaaldrich.com) at a 1:10000 dilution. Anti-rabbit or anti-mouse horseradish

peroxidase-conjugated antibodies (www.promega.com) were used as secondary antibodies. An ECL Prime Western Blotting Detection Reagent (RPN 2236, http://www.gelifesciences.com) was used for the development of the blot following the manufacturer's instructions; and signal was visualized using the ChemiDoc™ Touch Imaging System (www.bio-rad.com).

References.

Belda-Palazon B, Nohales MA, Rambla JL, Acena JL, Delgado O, Fustero S, Martinez MC, Granell A, Carbonell J, Ferrando A. 2014. Biochemical quantitation of the eIF5A hypusination in Arabidopsis thaliana uncovers ABA-dependent regulation. *Front Plant Sci* 5: 202.

Brandt R, Salla-Martret M, Bou-Torrent J, Musielak T, Stahl M, Lanz C, Ott F, Schmid M, Greb T, Schwarz M, et al. 2012. Genome-wide binding-site analysis of REVOLUTA reveals a link between leaf patterning and light-mediated growth responses. *Plant J* 72(1): 31-42.

Carabelli M, Sessa G, Baima S, Morelli G, Ruberti I. 1993. The Arabidopsis Athb-2 and -4 genes are strongly induced by far-red-rich light. *Plant J* 4(3): 469-479.

Cifuentes-Esquivel N, Bou-Torrent J, Galstyan A, Gallemi M, Sessa G, Salla Martret M, Roig-Villanova I, Ruberti I, Martinez-Garcia JF. 2013. The bHLH proteins BEE and BIM positively modulate the shade avoidance syndrome in Arabidopsis seedlings. *The Plant Journal* 75(6): 989-1002.

Chini A, Fonseca S, Chico JM, Fernandez-Calvo P, Solano R. 2009. The ZIM domain mediates homo- and heteromeric interactions between Arabidopsis JAZ proteins. *Plant J* 59(1): 77-87.

Formstecher E, Aresta S, Collura V, Hamburger A, Meil A, Trehin A, Reverdy C, Betin V, Maire S, Brun C, et al. 2005. Protein interaction mapping: a Drosophila case study. *Genome Res* 15(3): 376-384.

Fuse T, Sasaki T, Yano M. 2001. Ti-plasmid vectors useful for functional analysis of rice genes. Plant Biotechnology 18: 219-222.

Galstyan A, Cifuentes-Esquivel N, Bou-Torrent J, Martinez-Garcia JF. 2011. The shade avoidance syndrome in Arabidopsis: a fundamental role for atypical basic helix-loop-helix proteins as transcriptional cofactors. *Plant J* 66(2): 258-267.

Gallemi M, Galstyan A, Paulisic S, Then C, Ferrandez-Ayela A, Lorenzo-Orts L, Roig-Villanova I, Wang X, Micol JL, Ponce MR, et al. 2016. DRACULA2 is a dynamic nucleoporin with a role in regulating the shade avoidance syndrome in Arabidopsis. *Development* 143(9): 1623-1631.

Godoy M, Franco-Zorrilla JM, Perez-Perez J, Oliveros JC, Lorenzo O, Solano R. 2011. Improved protein-binding microarrays for the identification of DNA-binding specificities of transcription factors. *Plant J* 66(4): 700-711.

Graeff M, Straub D, Eguen T, Dolde U, Rodrigues V, Brandt R, Wenkel S. 2016. MicroProtein-Mediated Recruitment of CONSTANS into a TOPLESS Trimeric Complex Represses Flowering in Arabidopsis. *PLoS Genet* 12(3): e1005959.

Hellens RP, Edwards EA, Leyland NR, Bean S, Mullineaux PM. 2000. pGreen: a versatile and flexible binary Ti vector for Agrobacterium-mediated plant transformation. *Plant Mol Biol* 42(6): 819-832.

Höfgen R, Willmitzer L. 1990. Biochemical and genetic analysis of different patatin isoforms expressed in various organs of potato (Solanum tuberosum). Plant Sci 66: 221-230.

Kaufmann K, Wellmer F, Muino JM, Ferrier T, Wuest SE, Kumar V, Serrano-Mislata A, Madueno F, Krajewski P, Meyerowitz EM, et al. 2010. Orchestration of floral initiation by APETALA1. *Science* 328(5974): 85-89.

Li X. 2011. Infiltration of Nicotiana benthamiana Protocol for Transient Expression via Agrobacterium. *Bio-Protocol* Bio101: e95. http://www.bio-protocol.org/e95.

Martinez-Garcia JF, Gallemi M, Molina-Contreras MJ, Llorente B, Bevilaqua MR, Quail PH. 2014. The shade avoidance syndrome in Arabidopsis: the antagonistic role of phytochrome a and B differentiates vegetation proximity and canopy shade. *PLoS One* 9(10): e109275.

Martinez-Garcia JF, Virgos-Soler A, Prat S. 2002. Control of photoperiod-regulated tuberization in potato by the Arabidopsis flowering-time gene CONSTANS. *Proceedings of the National Academy of Sciences, USA* 99(23): 15211-15216.

Roig-Villanova I, Bou J, Sorin C, Devlin PF, Martinez-Garcia JF. 2006. Identification of primary target genes of phytochrome signaling. Early transcriptional control during shade avoidance responses in Arabidopsis. *Plant Physiology* 141(1): 85-96.

Schena M, Davis RW. 1992. HD-Zip proteins: members of an Arabidopsis homeodomain protein superfamily. *Proc Natl Acad Sci U S A* 89(9): 3894-3898.

Schena M, Lloyd AM, Davis RW. 1993. The HAT4 gene of Arabidopsis encodes a developmental regulator. *Genes Dev* 7(3): 367-379.

Sessa G, Morelli G, Ruberti I. 1993. The Athb-1 and -2 HD-Zip domains homodimerize forming complexes of different DNA binding specificities. *EMBO J* 12(9): 3507-3517.

Sorin C, Salla-Martret M, Bou-Torrent J, Roig-Villanova I, Martinez-Garcia JF. 2009. ATHB4, a regulator of shade avoidance, modulates hormone response in Arabidopsis seedlings. *The Plant Journal* 59(2): 266-277.

Wellmer F, Alves-Ferreira M, Dubois A, Riechmann JL, Meyerowitz EM. 2006. Genome-wide analysis of gene expression during early Arabidopsis flower development. *PLoS Genet* 2(7): e117.

Weng L, Dai H, Zhan Y, He Y, Stepaniants SB, Bassett DE. 2006. Rosetta error model for gene expression analysis. *Bioinformatics* 22(9): 1111-1121.